Semiconductors, Vol. 35, No. 9, 2001, pp. 997–1005. Translated from Fizika i Tekhnika Poluprovodnikov, Vol. 35, No. 9, 2001, pp. 1041–1049.

ELECTRONIC AND OPTICAL PROPERTIES OF SEMICONDUCTORS

Numerical Simulation of Intrinsic Defects in SiO_2 and Si_3N_4

V. A. Gritsenko*, Yu. N. Novikov*, A. V. Shaposhnikov*, and Yu. N. Morokov**

** Institute of Semiconductor Physics, Siberian Division, Russian Academy of Sciences, pr. Akademika Lavrent'eva 13, Novosibirsk, 630090 Russia*

*** Institute of Computational Technologies, Siberian Division, Russian Academy of Sciences, Novosibirsk, 630090 Russia*

Submitted February 14, 2001; accepted for publication February 15, 2001

Abstract—The electronic structure of major intrinsic defects in SiO_2 and Si_3N_4 was calculated by the MINDO/3 and the density-functional methods. The defects that are of interest from the standpoint of their ability to capture electrons or holes were considered; these centers include the three- and two-coordinated silicon atoms, the one-coordinated oxygen atom, and the two-coordinated nitrogen atom. The gain in energy as a result of capturing an electron or a hole with allowance made for electronic and atomic relaxation was determined for these defects. The experimental X-ray spectra for both materials are compared with calculated spectra. © *2001 MAIK "Nauka/Interperiodica".*

1. INTRODUCTION

Amorphous silicon oxide (a-SiO_2) and silicon nitride (a-Si_3N_4) are the most important insulating materials in modern microelectronics. The oxide has a low surface-state density at its boundary with silicon and high chemical stability and features low leakage currents and a high breakdown voltage [1]. Silicon nitride is used in masks during the diffusion of impurities into silicon and its oxidation and has a high concentration of electron and hole traps ($\sim 5 \times 10^{18}$ cm^{-3}) [2].

A reduction in the channel length of a metal–oxide–semiconductor (MOS) transistor is accompanied with a decrease in the gate-insulator thickness. An increase in the field in the channel leads to the heating of electrons and holes in the channel and to their injection into the insulator. The capture of electrons and holes by traps in the insulator results in the accumulation of charge in the insulator, a shift of the threshold voltage, the insulator breakdown, and the degradation of a MOS transistor.

Oxide–nitride–oxide (ONO) structures are widely used in silicon-based devices; these structures have a higher effective dielectric constant compared to silicon oxide. Silicon nitride is used as an active medium in the Si–SiO_2–Si_3N_4–SiO_2–Si memory structures. At present, the arrays of electrically programmable read-only memories (EPROMs) are being developed on the basis of ONO structures with a capacity of 10^{12} bit/chip. The lifetime of electrons and holes at the traps in Si_3N_4 is as long as ~10 years at 300 K. The silicon-based EPROMs replace the magnetic and optical memory media.

Many experimental and theoretical studies have been concerned with gaining insight into the identity of the traps (their atomic and electronic structure) in SiO_2 and Si_3N_4. However, only the origin of one type of trap has been identified so far. It has been shown that the oxygen vacancy in SiO_2 acts as a hole trap [3].

In this paper, we report the results of theoretical studies on the electronic structure of intrinsic defects in SiO_2 and Si_3N_4; the defects of interest from the standpoint of their ability to capture electrons or holes were considered. The main task consisted in determining the energy gain ΔE resulting from the capture of an electron or hole by the defect with allowance made for electronic and atomic relaxation. Calculations were performed by the MINDO/3 method and that based on the density-functional theory (DFT) in the cluster approximation. The MNDO method was used in a number of cases.

Calculations using the MINDO/3 method were performed in the approximation of the unrestricted Hartree–Fock method using the same parameters as were used previously [4, 5]. Calculations using the DFT method were performed using an ADF software package [6]. We used the double zeta basis of the Slater-type functions including the polarization functions for all atoms. We considered both the valence and shell electrons of atoms. Geometric parameters were optimized at the GGA level using the Becke formula for exchange interaction [7] and the Lee–Yang–Parr (LYP) formula for electronic correlation [8].

The α-quartz structure was used as the initial structure in forming the SiO_2 clusters; the β-Si_3N_4 structure was used in the case of silicon nitride. In all the clusters that were calculated, the dangling bonds of the boundary atoms were saturated with hydrogen atoms. For the clusters simulating the defects, the relaxation of atoms in the vicinity of the defect was taken into account for all charge states.

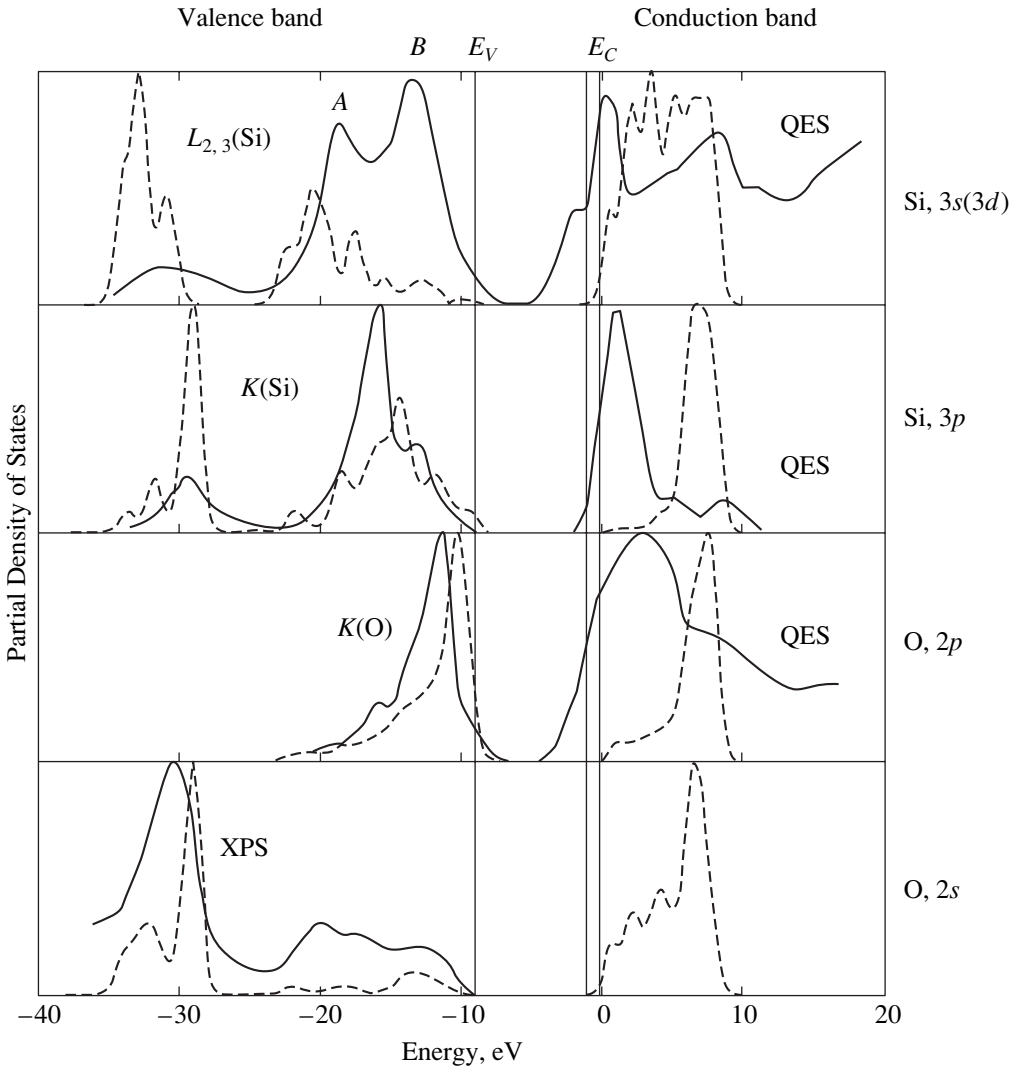

Fig. 1. Experimental X-ray emission spectra (solid lines) and the partial densities of states (dashed lines) calculated for atoms in the vicinity of the center of a $Si_{47}O_{52}H_{84}$ cluster that simulates the SiO_2 bulk.

The energy gain resulting from the capture of a hole or electron by the defect was calculated using the formula [9]

$$\Delta E^{h,e} = (E^0_{\text{vol}} + E^{\pm}_{\text{def}}) - (E^{\pm}_{\text{vol}} + E^0_{\text{def}}), \qquad (1)$$

where $E^{0,\pm}_{\text{vol}}$ and $E^{0,\pm}_{\text{def}}$ are the total energies of clusters that simulate the volume or defect in different charge states $(0, \pm 1)$.

Previously [10–12], the energy gain ("electrical level") for certain defects in SiO_2 was calculated by almost the same method, but the experimental values of the band edges (rather than their theoretical estimates) were used. However, in this case, it is necessary to take into account the polarization energy of the external medium in calculating the charged clusters, which was not carried out in [10–12]. If formula (1) is used, the polarization energy of the external medium for two charged clusters is reduced under the condition that clusters close in size are used for simulating the bulk and the defect. The difference is appreciable. The calculation of electron capture by the ≡SiO* defect in SiO_2 using the MINDO/3 method may serve as an example. The energy gain of $\Delta E = 1.44$ eV was reported in [11], whereas the calculation with formula (1) yields 2.3 eV.

2. ELECTRONIC STRUCTURE OF THE SiO_2 BULK

The electronic structure of silicon oxide has been considered by us previously [4]. In Fig. 1, the dashed lines represent the partial densities of one-electron states (PDOESs) calculated by the MINDO/3 method for a $Si_{47}O_{52}H_{84}$ cluster, which contains 183 atoms. All the PDOESs were calculated for the atoms located in the vicinity of the cluster center. The calculated PDOESs and the experimental spectra were normalized

to the maximum value (separately for the valence and conduction bands).

The solid lines in Fig. 1 represent experimental a-SiO_2 X-ray emission spectra (XES) $L_{2,3}$ (Si), K (Si), and K (O); the X-ray photoelectron spectrum (XPS, the lowest spectrum); and also the quantum-efficiency spectra (QES). These spectra have been reported previously [4]. The energy origin was taken equal to the electron energy in free space. The experimental positions of the edges of the E_C and E_V bands are indicated by vertical lines in Fig. 1.

It is typical that only the one-electron transitions are considered in interpreting the X-ray emission spectra. In this case, the intensities of the transitions allowed in the dipole approximation are proportional to the density of electronic states in the valence band and to the transition probability. If the transition matrix element depends only slightly on the energy, the XES approximately represent the PDOES in the valence band.

The plots represented in Fig. 1 show that the silicon dioxide valence band consists of two subbands separated by a gap. The lower narrow subband includes mainly the 2s oxygen states with a small addition of the 3s and 3p silicon states. The upper subband incorporates the 2p oxygen orbitals and the 3s and 3p silicon states. The valence-band top is mainly formed of $2p_\pi$ oxygen orbitals.

The $L_{2,3}$ (Si) XES represents the transitions from the Si 3s and 3d states to the 2p Si level. It is notable that the peak B in the vicinity of the valence-band top is not present in the calculated PDOES for the 3s Si state (see Fig. 1), although this peak is clearly pronounced in the experimental spectrum. This is characteristic of all calculations that use only the 3s- and 3p-silicon basis functions [4]. A similar situation occurs in silicon nitride [5].

It has been shown in a number of studies (see, for example, [13, 14]) that the 3d silicon state can make an appreciable contribution to the B peak. However, from a general standpoint, the $L_{2,3}$ (Si) spectrum is caused by transitions of electrons to the 2p Si state from the bulk-related extended states rather than from purely atomic states [5]. The transitions from the Si 3d and 4s states contribute to peak B, as do non-single-center transitions of electrons to the 2p Si states from the atomic 2p states of the nearest oxygen atoms.

We calculated the X-ray emission spectra using the DFT method and taking into account both the one- and two-center transitions. The emission spectra corresponding to one-center transitions have been calculated previously [13] using the self-consistent pseudopotential method.

In order to simulate the SiO_2 bulk by the DFT method, we used a 33-atom $Si_5O_{16}H_{12}$ cluster that was centered around the silicon atom and included three regular coordination spheres of the oxide.

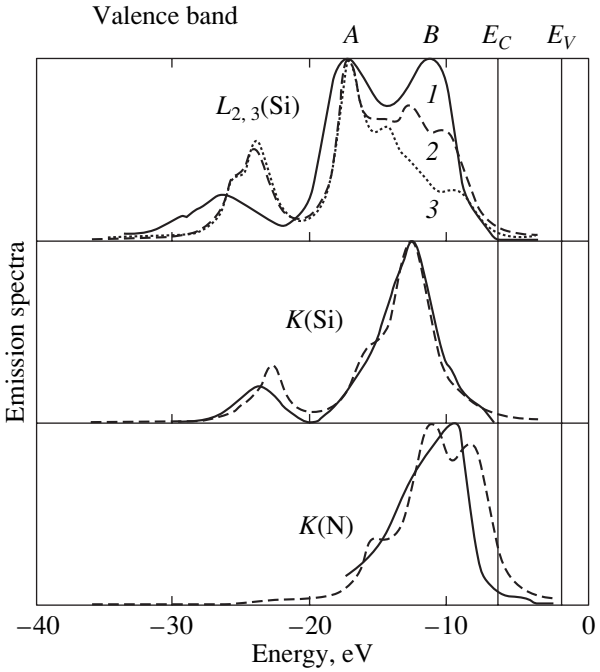

Fig. 2. The X-ray emission spectra for silicon oxide. Experimental spectra are represented by solid lines. The spectra calculated by the DFT method for a $Si_5O_{16}H_{12}$ cluster are shown by the dashed lines if the polarized 3d Si functions were used in the calculations and by the dotted line if these functions were not used.

The results of these calculations are compared with experimental spectra in Fig. 2. All the curves were separately normalized to a unit peak height; theoretical curves were shifted along the energy scale in order to ensure the coincidence of the calculated and experimental peaks (for the $L_{2,3}$ (Si) spectrum, the coincidence with peak A was ensured). The transition intensities were calculated in the frozen-orbital approximation: both the initial state (a hole at the inner orbital) and the final state (a hole in the valence band) were composed of molecular orbitals obtained as a result of the same calculation of the ground neutral state. The transition energies were assumed to be equal to the difference between the corresponding one-electron energies (thus, Koopmans' theorem was used). The matrix elements of transitions were calculated in the dipole approximation.

The theoretical curves represented in Fig. 2 were calculated with the introduction of the polarized Si 3d functions, except for curve *3* in the $L_{2,3}$ (Si) spectrum, which was calculated without introducing the above functions. Thus, the calculations indicate that the polarized 3d functions of Si contribute appreciably to peak B.

The experiment gives no way of separating the contributions of antibonding and bonding 2p oxygen states. However, it is important that the 3p Si states and, consequently, the related 2p O states are observed up to the

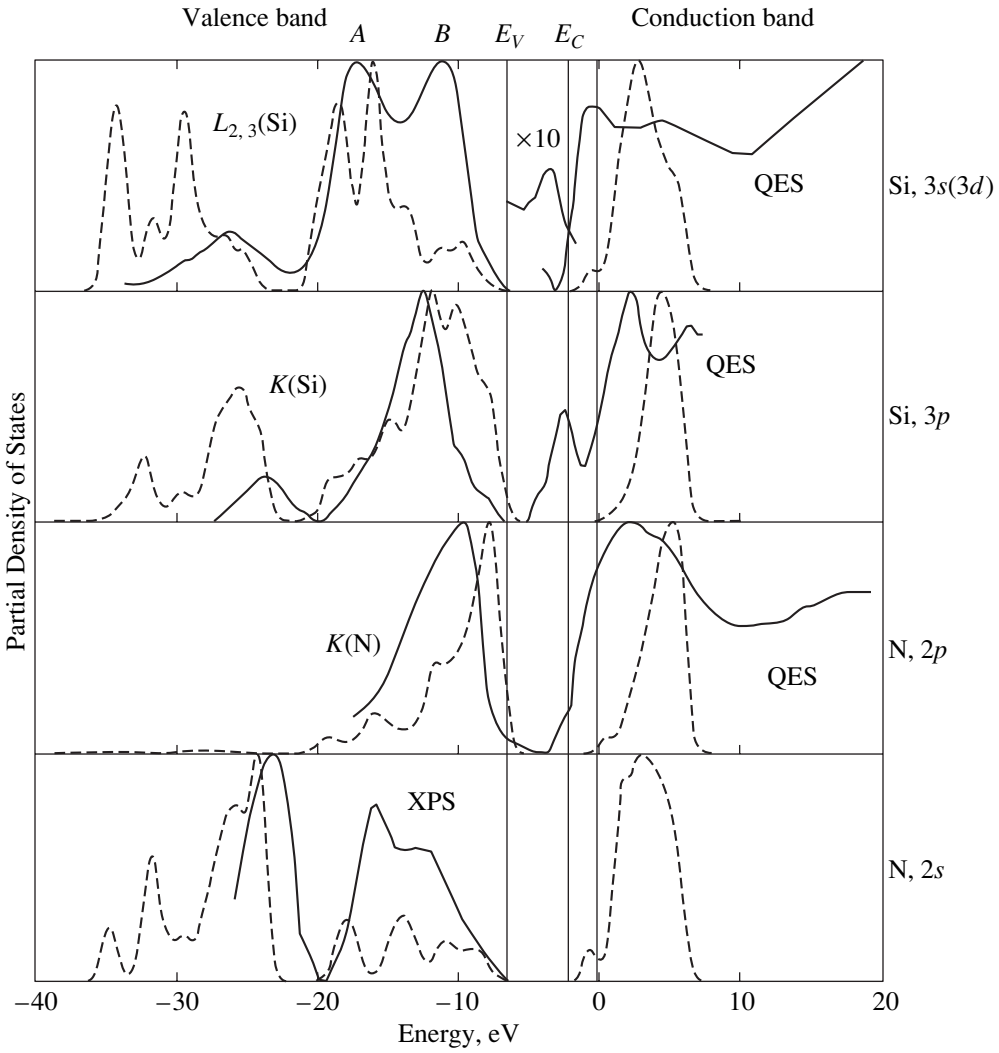

Fig. 3. Experimental X-ray emission spectra (the solid lines) and the partial densities of states (the dashed lines) calculated for the atoms near the center of a $Si_{61}N_{74}H_{76}$ cluster that simulates the Si_3N_4 bulk.

valence-band top. This means that not only the antibonding $2p_\pi$ O states but also the weakly bonding $2p$(O)–$3s,3p,3d$(Si) states exist in the upper part of the valence band. It has been argued [4] that this corresponds to the presence of the light and heavy holes in SiO_2. This assertion is based on the assumption that the rapid transport of holes in SiO_2 is accomplished via transport over the Si–O–Si bonds rather than via hops between the antibonding $2p_\pi$ orbitals of oxygen atoms.

3. ELECTRONIC STRUCTURE OF THE Si_3N_4 BULK

Electronic structures of the Si_3N_4 bulk have been considered previously [5]. The results of calculating the energy-band structure for the α and β phases of silicon nitride were reported, for example, by Xu *et al.* [14].

Figure 3 shows the PDOESs calculated for a $Si_{61}N_{74}H_{76}$ 211-atom cluster. Both the calculations and experimental data indicate that the Si_3N_4 valence band consists of two subbands. The lower narrow band is mainly formed by the $2s$ nitrogen orbitals, whereas the upper wide band is formed by the $2p$ nitrogen orbitals, which overlap the $3s$ and $3p$ silicon orbitals. The valence-band top is mainly formed by the nitrogen $2p_\pi$ orbitals.

Peak *B* in the upper part of the valence band in the $L_{2,3}$ (Si) spectrum (Fig. 3) has the same origin [5] as that of the peak *B* for SiO_2 considered above. This is supported by the DFT calculations of the Si_3N_4 emission spectra shown in Fig. 4.

In the vicinity of the Si_3N_4 valence-band top, a narrow band of antibonding $2p_\pi$ nitrogen orbitals is found. In addition, there is a nonzero density of states formed by the bonding $3s,3p,3d$(Si)–$2p,2s$(N) orbitals; holes with higher mobility may correspond to this density of states. The energy-band calculations yield a high

anisotropy of the effective mass of holes, both for SiO_2 and Si_3N_4 [14]. An appreciable component of the hole effective mass is attributed to unshared pairs localized at the $2p_\pi$ (N) or $2p_\pi$ (O) orbitals.

4. ELECTRONIC STRUCTURE OF TRAPS IN SiO_2

At present, the models of defects responsible for the localization of electrons and holes in SiO_2 continue to be discussed intensively [15–18].

4.1. The Three-Coordinated Silicon Atom O_3≡Si (the E' Center)*

The main paramagnetic defect in SiO_2 is an oxygen vacancy that has captured a hole [1, 10, 17–20]. The atoms closest to the vacancy experience an asymmetric relaxation, and an unpaired electron is mainly localized at one of two three-coordinated silicon atoms. It has been assumed that the O_3≡Si* group in this defect gives rise to transitions in the absorption spectra in the vicinity of 5.8 eV [17, 20, 21]. Several types of paramagnetic *E*' centers are recognized in relation to different atomic surroundings of the O_3≡Si* group [17, 20, 21].

The basic clusters used to simulate the defects in SiO_2 are represented in Fig. 5. In order to simulate an isolated ≡Si* defect, we used a $Si_4O_{12}H_9$ 25-atom cluster that was centered at a three-coordinated silicon atom and included three coordination shells of the oxide atoms. The defect is paramagnetic in its neutral state. Calculations by the MINDO/3 method have shown that 47% of the spin density of an unpaired electron is localized at the three-coordinated silicon atom and 25% is localized at the three nearest oxygen atoms.

The neutral defect introduces a one-electron level into the band gap; this level is located at 3.5 eV above the "cluster" valence-band top (the last but one occupied level). In publications, Koopmans' theorem has been often used to estimate the energies of capture of an electron or hole by a defect. However, Koopmans' theorem may give rise to large errors for highly localized states. Thus, our use of a more consistent (Δ*SCF*) method expressed by formula (1) yielded an energy gain of 2.9 eV for electron capture by the ≡Si* defect, which is lower than the value estimated above using Koopmans' theorem by 0.6 eV. The energy gain as a result of the capture of an electron by the isolated ≡Si* defect was equal to 1.4 eV.

4.2. Two-Coordinated Silicon Atom ≡Si: (a Sililene Center)

This defect in SiO_2 is often related to the absorption band peaked at 5.0 eV and to luminescence bands peaked at 2.7 and 4.4 eV [18, 22–24].

In order to simulate this defect, we used a $Si_3O_8H_6$ 17-atom cluster, which was obtained from a $Si_5O_{16}H_{12}$ cluster that simulated the oxide bulk by breaking two Si–O bonds of the central silicon atom and by removing the two corresponding groups of atoms.

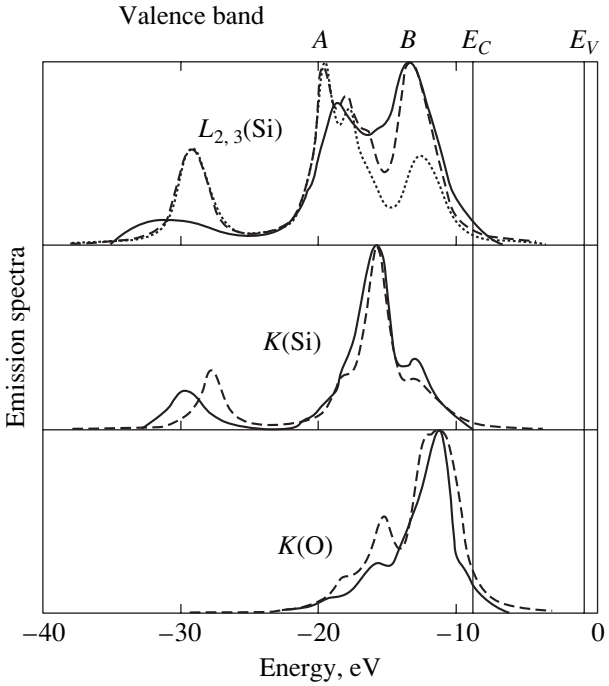

Fig. 4. X-ray emission spectra for silicon nitride. Experimental spectra are shown by solid lines. The spectra calculated by the DFT method for a $Si_{19}N_{26}H_{36}$ cluster are shown by dashed lines if the polarized 3*d* Si functions were used in the calculations and by the dotted line if these functions were not used.

Calculations show that the defect is diamagnetic in the neutral state. Two electrons of a two-coordinated silicon atom form an unshared pair that resides at the hybrid orbital lying in the O–Si–O plane. In calculations employing the MINDO/3 method, this hybrid orbital consists of 61% of the *s* atomic orbitals and 39% of *p* atomic orbitals of the silicon atom. Hole capture at this orbital transforms the defect into a paramagnetic state. As a result, 60% of the spin density becomes localized at the two-coordinated silicon atom. Calculations of the positively charged state performed by Dianov *et al.* [12] by the MNDO method indicated that 70% of the spin density is localized at the two-coordinated silicon atom.

The calculations employing the MINDO/3 method show that this defect is a trap for holes with a capture energy of about 1.5 eV. The calculation employing the DFT method shows that this defect is a hole trap with ΔE = 3.2 eV. The calculation employing the MNDO method yields a hole-capture energy of ΔE = 3.9 eV. No electrons are captured by this defect.

The ability of the =Si: defect to capture a hole indicates that this defect, in addition to the oxygen vacancy,

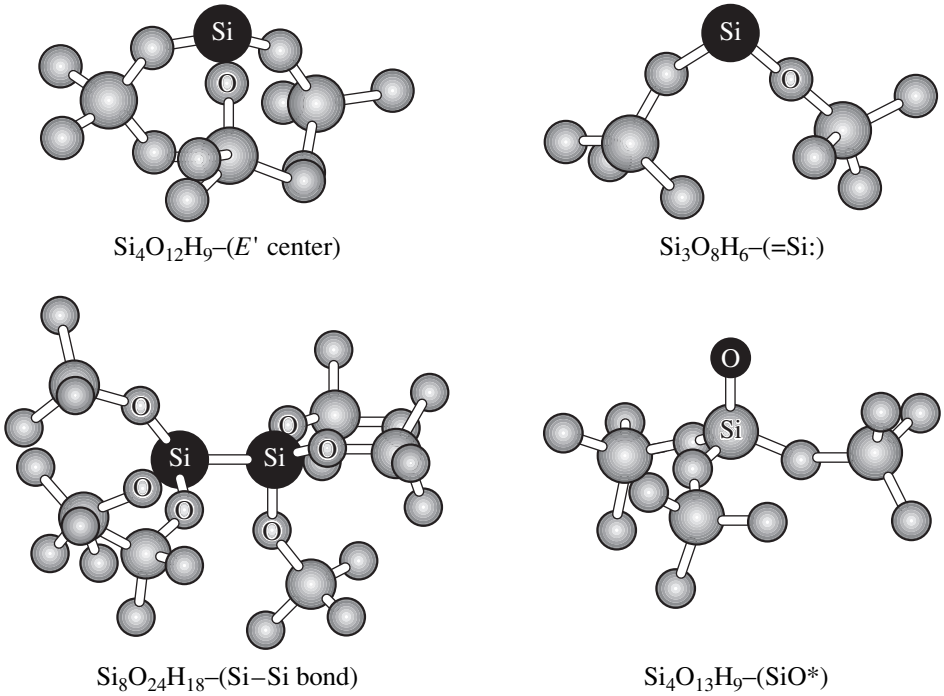

Fig. 5. Clusters used to simulate the defects in silicon oxide. Hydrogen atoms are not shown. The atoms forming defects are represented by shaded circles.

may be responsible for the accumulation of positive charge in the MOS devices subjected to radiation.

4.3. Silicon–Silicon Bond ≡Si–Si≡, Oxygen Vacancy

Experiments and theoretical calculations have shown that a neutral oxygen vacancy can capture a hole and, thus, give rise to the *E*' paramagnetic center [1, 10, 11, 18, 20]. The absorption band peak observed at 7.6 eV is typically related to the oxygen vacancy [17, 18]. It is assumed that the transition occurs between the bonding and antibonding states of the Si–Si bond formed.

As an initial cluster for forming the Si–Si bond, we chose a Si_8O24H_{18} 50-atom cluster that simulated an oxygen vacancy in the dioxide. The remote oxygen atom formed an angle of 144° with two neighboring silicon atoms. The $Si_8O_{24}H_{18}$ cluster consisted of two 25-atom halves, the distance between which was varied along the Si–Si bond. By choosing the distance L between these two halves, we then optimized the two silicon atoms in the Si–Si bond, with the positions of all other atoms remaining unchanged. The oxygen vacancy in dioxide corresponds to the initial distance of L = 3.1 Å. Calculations using the MINDO/3 method showed that, for L = 2.35 Å, this defect is an electron trap with ΔE = 1.0 eV. A hole can be also captured with ΔE = 3.0 eV. As the distance L increases, the gain in energy as a result of capturing an electron increases to 1.4 eV, which corresponds to an isolated ≡Si* defect. The gain in energy as a result of capturing a hole is virtually independent of the distance L.

The structure of neutral and positively charged oxygen vacancies has been theoretically studied in [10, 12, 18]. Snyder *et al.* [10] used several semiempirical methods: MINDO/3, MNDO, AM1, and PM3. A comparison of the results obtained by these methods shows that the MINDO/3 method is preferable [10]. The calculations yielded two local energy minima in the relaxation of the positively charged vacancy. One of the minima corresponds to an almost symmetric relaxation of atoms with a nearly symmetric electronic structure. The other minimum is deeper than the first one by 0.17 eV (MINDO/3). The transition to this state corresponds to an increase in the energy gain to 3.2 eV, which occurs when a hole is captured by an oxygen vacancy. This second minimum corresponds to the transfer of a silicon atom through the plane formed by three oxygen atoms bonded to the above silicon atom, with an accompanying formation of a weak bond with another (more remote) oxygen atom. The barrier height for such a transition is 0.4 eV (MINDO/3). An unpaired electron is localized at another three-coordinated silicon atom. Experiments with electron spin resonance (ESR) have shown that an unpaired electron is almost completely localized at a single silicon atom [20].

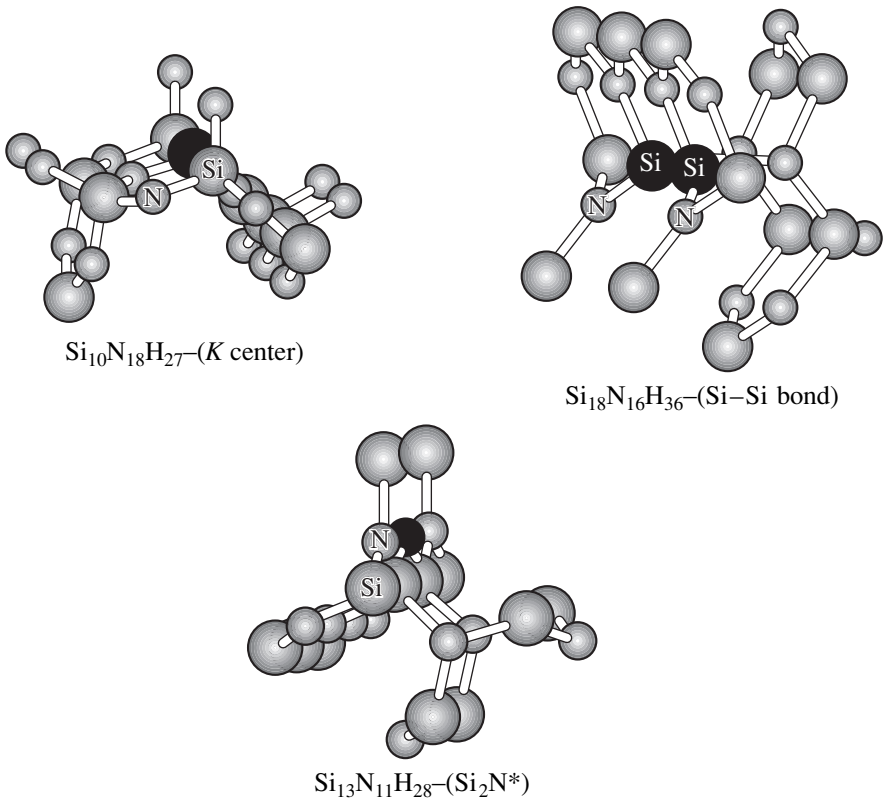

Fig. 6. The clusters used in simulating the defects in silicon nitride.

4.4. One-Coordinated Oxygen Atom ≡SiO (a "Nonbridging" Oxygen Atom)*

In order to reduce the amount of positive charge trapped in SiO_2, an empirical method has been developed; this method consists in the compensation of the above charge by a positive charge captured by electron traps, which are formed as a result of the wet oxidation of silicon [25]. However, the nature of such electron traps has not been clarified yet. It is believed that this electron trap may be attributed to a center that corresponds to the red luminescence line peaked at 1.9 eV and is related to the ≡SiO* defect [26]. This identification is supported by quantum-chemical calculations [17, 18]. It is assumed that this defect is responsible for the radiation resistance of oxide produced by wet oxidation.

In order to simulate a one-coordinated oxygen atom ≡SiO*, we used a $Si_4O_{13}H_9$ 26-atom cluster obtained from a "bulk" $Si_5O_{16}H_{12}$ cluster by breaking the outer O–Si bond of an oxygen atom in the first coordination sphere and by removing the corresponding atomic group.

The calculations using the MINDO/3 method [27] showed that this defect is only a trap for electrons with an energy gain of 2.3 as a result of electron capture. The defect is paramagnetic in its neutral state. An unpaired electron is localized at the $2p_\pi$ orbital of a one-coordinated oxygen atom. The calculation using the DFT method showed that the ≡SiO* defect is an electron trap with ΔE = 3.9 eV. The calculation by the MNDO method yields the value of the capture energy ΔE equal to 3.2 eV.

Thus, the three simulation methods that we considered verify the ability of the ≡SiO* defect to capture an electron; therefore, this defect may be used to interpret the electron traps with energies of 2.4–2.5 eV, which are observed in experiments with oxide depolarization [28].

5. ELECTRONIC STRUCTURE OF TRAPS IN Si_3N_4

Amorphous silicon nitride and oxynitride are considered to be alternatives to silicon oxide in silicon devices for the near future [29]; *a*-Si_3N_4 has a high concentration ($\sim 5 \times 10^{18}$ cm^{-3}) of electron and hole traps. It is believed that the capture of electrons and holes in *a*-Si_3N_4 is related to the defects induced by excess silicon atoms [30, 31]. The ESR signal was not detected either in the initial *a*-Si_3N_4 samples or in the samples subjected to the injection of electrons and holes [30, 31].

5.1. Three-Coordinated Silicon Atom N_3≡Si (the K Center)*

In order to simulate this defect, we used a $Si_{10}N_{18}H_{27}$ 55-atom cluster that is centered at the three-coordinated silicon atom and includes the atoms of three coordination shells of silicon nitride. The main clusters used in simulating the defects in Si_3N_4 are represented in Fig. 6.

Calculations by the MINDO/3 method show that an isolated ≡Si* defect captures an electron with an energy gain of 1 eV. The energy gain as a result of capturing a hole amounts to a mere 0.1 eV, which is within the model's error. The ≡Si* defect, which is paramagnetic in the neutral state, becomes diamagnetic after capturing an electron (a hole).

The absence of an ESR signal in the initial *a*-Si_3N_4 samples indicates that there are in fact no neutral isolated ≡Si* defects in these samples. In order to explain the absence of an ESR signal, it has been assumed that a pair of neutral defects ≡Si* gives rise to a pair of charged defects: ≡Si: and ≡Si* (the K^- and K^+ centers) as a result of the following reaction:

$$\equiv Si^* + \equiv Si^* \longrightarrow \equiv Si: + \equiv Si. \quad (2)$$

This model of "negative correlation energy" [30, 32, 33] implies that the energy gain ($-U$) is attained owing to the lattice relaxation.

We used the MINDO/3 method to calculate the characteristics of this defect in various charge states with allowance made for the relaxation of only the three-coordinated silicon atom. These calculations show that reaction (2) corresponds to the positive correlation energy equal to 4.0 eV. Nonempirical calculations at a level of 6-3G*/MP2 for a $Si(NH_2)_3$ 10-atom cluster yield a correlation energy of ~5.5 eV. Taking into account the polarization energy of the external medium according to the "classical model" [34], we obtain the following estimates for the correlation energy U: +2.7 eV (MINDO/3) and +3.5 eV (*ab initio*).

Recent DFT-based calculations for reaction (2) [34] yielded a positive correlation energy of $U = +0.9$ eV for isolated ≡Si* defects in silicon nitride. This comparatively small value is accounted for by a pronounced relaxation effect observed [34] for the positively charged ≡Si defect.

Thus, the calculations do not support the widely accepted model of negative correlation energy for the *K* centers in *a*-Si_3N_4.

5.2. Silicon–Silicon Bond ≡Si–Si≡, the Nitrogen Vacancy

The ≡Si–Si≡ defects can be most easily formed in the silicon nitride bulk by introducing a nitrogen vacancy. The latter was simulated using a $Si_{18}N_{16}H_{36}$ 70-atom cluster centered at the nitrogen atom to be removed.

As follows from calculations using the MINDO/3 method, a nitrogen vacancy serves as a trap for electrons ($\Delta E = 1.6$ eV) and holes ($\Delta E = 1.0$ eV). In its neutral state, the defect is paramagnetic. When a hydrogen atom is trapped by this defect, a dangling bond of one of the silicon atoms becomes saturated. The capture of an electron by such a center is accompanied by the dissociation of the Si–H bond and by the escape of the hydrogen atom to the nitride bulk. As a result, the total energy gain amounts to about 1 eV.

If a three-coordinated silicon atom (together with other atoms bonded to it) is removed from a $Si_{18}N_{16}H_{36}$ cluster, we obtain a $Si_{14}N_{12}H_{30}$ 56-atom cluster, which may be considered as a model of the Si–Si bond with an initial 2.9-Å distance between silicon atoms. Such a defect is an electron trap with $\Delta E = 1.76$ eV. The capture of a hole is unlikely because a small electron-capture energy of $\Delta E = 0.34$ eV may be related to errors in the model.

*5.3. Two-Coordinated Nitrogen Atom $(\equiv Si)_2N$**

Experimental data reported by Yount and Lenahan [35] indicate that the $(\equiv Si)_2N^*$ is an electron trap in silicon oxynitride. In order to eliminate the electron traps in the gate oxynitride of silicon devices, the oxynitride is repeatedly oxidized. Assuming in this situation that the electron traps are $(\equiv Si)_2N^*$ defects, we may easily explain the elimination of the traps in this technological stage by the replacement of a two-coordinated nitrogen atom by a regularly coordinated oxygen atom [27].

The $(\equiv Si)_2N^*$ defect was simulated using a $Si_{13}N_{11}H_{28}$ cluster that incorporated the coordination shells of nitride atoms. Calculations by the MINDO/3 method indicate that this defect is an electron trap with $\Delta E = 0.8$ eV and acts as a hole trap only in silicon oxynitride enriched with oxygen [27]. The ability of the $(\equiv Si)_2N^*$ defect to trap an electron is corroborated by the recent DFT-based calculations [34]. In its neutral state, this defect is paramagnetic. The unpaired electron is localized at the $2p_\pi$ state of the nitrogen atom, which is consistent with the ESR data [20, 35].

6. CONCLUSION

In order to identify the traps in SiO_2 and Si_3N_4, we used quantum-chemical methods to calculate the energy gain that results from the major intrinsic defects in these materials trapping an electron or a hole. The calculations were performed in the cluster approximation with allowance made for electronic and atomic relaxation. It is shown that the ≡Si* defects, oxygen vacancies, and the ≡SiO* centers are electron traps in SiO_2, whereas the ≡Si*, nitrogen vacancies, and the $(\equiv Si)_2N^*$ centers act as electron traps in silicon nitride. The hole traps are ≡Si*, oxygen vacancies, and the (=Si:) defect in SiO_2; in Si_3N_4, the nitrogen vacancy acts as a hole trap.

ACKNOWLEDGMENTS

This study was supported by INTAS, grant no. 97-0347.

REFERENCES

1. V. A. Gritsenko, *Structure and Electronic Properties of Amorphous Insulators in Silicon MIS-Devices* (Nauka, Novosibirsk, 1993).
2. *Silicon Nitride in Electronics*, Ed. by A. V. Rzhanov (Nauka, Novosibirsk, 1982; Elsevier, New York, 1988).
3. P. M. Lenahan and P. V. Dressendorfer, J. Appl. Phys. **55**, 3495 (1984).
4. V. A. Gritsenko, R. M. Ivanov, and Yu. N. Morokov, Zh. Éksp. Teor. Fiz. **108**, 2216 (1995) [JETP **81**, 1208 (1995)].
5. V. A. Gritsenko, Yu. N. Morokov, and Yu. N. Novikov, Fiz. Tverd. Tela (St. Petersburg) **39**, 1342 (1997) [Phys. Solid State **39**, 1191 (1997)].
6. C. Fonseca Guerra, J. G. Snijders, G. te Velde, and E. J. Baerends, Theor. Chem. Acc. **99**, 391 (1998).
7. A. D. Becke, Phys. Rev. A **38**, 3098 (1988).
8. C. Lee, W. Yang, and R. G. Parr, Phys. Rev. B **37**, 785 (1988).
9. A. X. Chu and W. B. Fowler, Phys. Rev. B **41**, 5061 (1990).
10. K. C. Snyder and W. B. Fowler, Phys. Rev. B **48**, 13238 (1993).
11. A. H. Edwards and W. B. Fowler, in *Structure and Bonding in Noncrystalline Solids*, Ed. by G. E. Walrafen and A. G. Revesz (Plenum, New York, 1986), p. 139.
12. E. M. Dianov, V. O. Sokolov, and V. B. Sulimov, J. Non-Cryst. Solids **149**, 5 (1992).
13. A. Simunek, J. Vackar, and G. Wiech, J. Phys.: Condens. Matter **5**, 867 (1993).
14. Y.-N. Xu and W. Y. Ching, Phys. Rev. B **51**, 17379 (1995).
15. G. Pacchioni and M. Vitiello, J. Non-Cryst. Solids **245**, 175 (1999).
16. V. A. Gritsenko, J. B. Xu, R. W. M. Kwok, *et al.*, Phys. Rev. Lett. **81**, 1054 (1998).
17. L. Skuja, J. Non-Cryst. Solids **239**, 16 (1998).
18. G. Pacchioni and G. Ierano, Phys. Rev. B **57**, 818 (1998).
19. A. R. Silin' and A. N. Trukhin, *Point Defects and Elementary Excitations in Crystalline and Vitreous SiO_2* (Zinatne, Riga, 1985).
20. W. L. Warren, E. H. Poindexter, M. Offenberg, and W. Muller-Warmuth, J. Electrochem. Soc. **139**, 872 (1992).
21. D. L. Griscom, J. Non-Cryst. Solids **73**, 51 (1985).
22. V. A. Radzig, J. Non-Cryst. Solids **239**, 49 (1998).
23. G. Pacchioni and R. Ferrario, Phys. Rev. B **58**, 6090 (1998).
24. V. A. Gritsenko, Yu. G. Shavalgin, P. A. Pundur, *et al.*, Microelectron. Reliab. **39**, 715 (1999).
25. Z. Shanfield and M. M. Moriwaki, IEEE Trans. Nucl. Sci. **NS-31**, 1242 (1984).
26. L. Skuja, J. Non-Cryst. Solids **179**, 51 (1994).
27. Yu. N. Morokov, Yu. N. Novikov, V. A. Gritsenko, and H. Wong, Microelectron. Eng. **48**, 175 (1999).
28. V. J. Kapoor, F. J. Feigl, and S. R. Butler, J. Appl. Phys. **48**, 739 (1977).
29. Y. Shi, X. Wang, and T.-P. Ma, IEEE Trans. Electron Devices **46**, 362 (1999).
30. W. L. Warren, J. Kanichi, J. Robertson, *et al.*, J. Appl. Phys. **74**, 4034 (1993).
31. V. A. Gritsenko and A. D. Milov, Pis'ma Zh. Éksp. Teor. Fiz. **64**, 489 (1996) [JETP Lett. **64**, 531 (1996)].
32. P. W. Anderson, Phys. Rev. Lett. **34**, 953 (1975).
33. R. A. Street and N. F. Mott, Phys. Rev. Lett. **35**, 1293 (1975).
34. G. Pacchioni and D. Erbetta, Phys. Rev. B **61**, 15005 (2000).
35. J. T. Yount and P. M. Lenahan, J. Non-Cryst. Solids **164-166**, 1069 (1993).

Translated by A. Spitsyn